ACADEMIC PRESS

Available online at www.sciencedirect.com

SCIENCE DIRECT®

Analytical Biochemistry 315 (2003) 95–105

ANALYTICAL BIOCHEMISTRY

www.elsevier.com/locate/yabio

# Quantitation of gene expression in neural precursors by reverse-transcription polymerase chain reaction using self-quenched, fluorogenic primers

Brian Lowe,[a] Herbert A. Avila,[b] Fredric R. Bloom,[b] Martin Gleeson,[c] and Wolfgang Kusser[c,*]

[a] *Invitrogen Corporation, 7300 Governors Way, Frederick, MD 21704, USA*
[b] *Anhydrocyte, Inc., 9700 Great Seneca Highway, Rockville, MD 20850, USA*
[c] *Invitrogen Corporation, 1610 Faraday Avenue, Carlsbad, CA 92008, USA*

Received 4 October 2002

**Abstract**

Quantitative RT-PCR using LUX primers was performed to determine the expression patterns of various transcripts in samples of pluripotent, mouse P-19 stem cells. The P-19 cells were used because they transform into neuron-like cells upon retinoic acid treatment. The expression of neural and stem cell genes, including GLUR1, GABA-B1a, NMDA1, GAP-43, ChAT, BDNF, nestin, BMP-2, BMP-4, and EGR1, was increased, approximately 10- to 1000-fold, during the course of differentiation from 0 to 11 days after induction with retinoic acid. A 3-fold serial dilution of in vitro-transcribed ChAT mRNA from 66 to $10^7$ copies was discriminated by qRT-PCR using fluorogenic LUX primers. Results of quantitation using PCR utilizing dual LUX primer pairs were similar to quantitation using single LUX primers, and to results derived by using an alternate method for qRT-PCR, the 5′-nuclease probe assay. The efficiencies of PCRs using various primer sets were similar, so that a comparative $C_T$ method of quantifying relative amounts of transcripts was performed. We conclude that real-time RT-PCR using fluorogenic LUX primers is a reliable, effective alternative to present methods for quantifying several transcripts in neural stem cells.
© 2003 Elsevier Science (USA). All rights reserved.

*Keywords:* LUX primers; RT-PCR; Real-time; Expression; Neural precursors; P-19

The importance of investigating the role of gene expression in neural stem cells has increased due to the possible use of stem cells as donor cells for use in nervous system repair [1–3]. Neural stem cells undergo complex changes in gene expression during their differentiation. The expression of mRNA in these cells may be quantified using the traditional Northern blot analysis, RNase protection [4], in situ hybridization [5], or competitive RT-PCR[1] [6,7]. These methods are time consuming and require considerable effort. Gene microarray [8], SAGE [9], and differential display [10] are newer methods that are efficiently able to track the expression of multiple genes, but they are complicated and require large amounts of sample material. Fluorescence-based, real-time PCR proves to be a sensitive, reliable, and convenient alternative for quantifying the changes in expression of multiple genes [11–13]. Real-time PCR requires small sample size and is adaptable to automated, high-throughput sample assays.

A fluorescence-based, real-time PCR technique that utilizes a fluorogenic primer labeled only with a single fluorophore was recently developed as a cost-effective alternative to other fluorescence-based PCR techniques [14,15]. These other techniques, such as TaqMan probe, Molecular Beacon, Ampliflour, DNA-binding dyes (SYBR green), and others are more studied than this newer method and may be reviewed elsewhere

* Corresponding author.
*E-mail address:* wolfgang.kusser@invitrogen.com (W. Kusser).

[1] *Abbreviations used:* RT-PCR, reverse-transcription polymerase chain reaction; FAM, 5 or 6-carboxyfluorescein; JOE, 6-carboxy-4′, 5′-dichloro-2′, 7′-dimethoxyfluorescein; ChAT, choline acetyltransferase; qPCR, quantitative PCR.

0003-2697/03/$ - see front matter © 2003 Elsevier Science (USA). All rights reserved.
doi:10.1016/S0003-2697(02)00695-4

[16–22]. The fluorogenic primer method, however, has some advantages over some methods that include the ease of design and synthesis of the fluorogenic primers. Other advantages and disadvantages are listed in previous works [14,15]. The fluorogenic primer is designed to be "self-quenched" until it is incorporated into a double-stranded PCR product, whereupon its fluorescence increases, i.e., is "dequenched." The fluorogenic primer is called a LUX primer, meaning Light-Upon-eXtension. The counterpart PCR primer used in conjunction with the fluorogenic primer is a standard, unlabeled oligonucleotide. LUX primer design is based on studies that demonstrate the effects of the primary and secondary structure of oligonucleotides on the emission properties of a conjugated fluorophore [15]. The design factors are largely based on the necessity of having guanosine bases in the primary sequence nearby the conjugated fluorophore. The fluorophore may be various commonly used dyes such as FAM (5 or 6-carboxyfluorescein) and JOE (6-carboxy-4′, 5′-dichloro-2′, 7′-dimethoxyfluorescein). Furthermore, the LUX primers have a nonsequence-specific 5′-tail that is complementary to the 3′-end of the primer. The 5′-tail enables the primer to assume a hairpin conformation at temperatures below the melting point of the hairpin, and it also effects the fluorescence of the LUX primer. The above characteristics and other standard characteristics of the primers, such as length and $T_m$, are included in the primer design by proprietary software, called LUX Designer (Invitrogen, http://www.invitrogen.com/lux). These design rules enable the software to output numerous primer pairs that are located throughout the target (input) sequence.

We, here, develop a useful model system for investigating neural stem cell expression. The pluripotent P-19 mouse carcinoma cell line was used because it is well characterized and convenient [23–25]. Gene expression was analyzed in P-19 cells during differentiation by using the newly devised real-time LUX PCR method. In order to validate our methods, the genes that were selected for analysis were ones for which the pattern of expression was previously known to some extent. To further validate our method, we compared gene expression results obtained using the fluorogenic-primer method with those obtained using a more traditional, 5′-nuclease assay [18,19]. We demonstrate that several important genes involved with P-19 cell differentiation may be rapidly quantified using the fluorogenic primer technique. Our gene expression data are consistent with previous studies using other methods, and, in some cases, provide relative quantitation values not performed in previous qualitative studies. Furthermore, we provide quantitative expression data for select genes over a more extensive period of differentiation than some studies, and provide some data that are not found elsewhere.

## Materials and methods

### *Cell culture*

P-19 mouse embryonic carcinoma cells (American Type Culture Collection, CRL 1825, Manassas, VA) were cultured in standard growth medium (α-MEM, 7.5% donor calf, and 2.5% fetal bovine serum; Gibco, Grand Island, NY). P-19 cells were induced to differentiate into neuronal-like cells [25] by seeding them ($1 \times 10^6$ cells/100-mm nonadhesive dish) into Differentiation medium containing Neurobasal medium, 2% B27 supplement, 0.5 mM L-glutamine (Gibco), and 50 nM retinoic acid (Sigma, St. Louis, MO).

### *Templates*

RNA was isolated from P-19 cells using the Trizol reagent (Invitrogen, Carlsbad, CA) as instructed by the vendor. Mouse brain and liver RNA samples were a generous gift of Mark Smith of Invitrogen or obtained from Stratagene (Catalog Nos. 776001 and 776009, La Jolla, CA).

Choline acetyltransferase (ChAT) mRNA was transcribed in vitro from cDNA templates using T7 RNA polymerase (Invitrogen). Full-length ChAT cDNA was amplified from P-19 cell RNA using primers bearing topoisomerase I recognition sites (forward, 5′-cggaacaa gggggctgctgggatctgg; reverse, 5′-tgagtcaagggctgagacggcg gaaatta). A 5′ T7 promoter and a 3′ poly(A) tail were joined to the cDNA by incubating the cDNA at 25 °C for 5 min in reactions containing topoisomerase-charged Topo Tools (Invitrogen), 5′ T7 element (No. T301-20) and 3′ poly(A) element (No. T307-20). The molar ratio of cDNA was 2× that of each element. An antibody-based "hotstart," proofreading *Taq* DNA polymerase mixture (Part No. 11304011, Invitrogen), was used to amplify full-length cDNA, and to amplify the linear cDNA construct after topoisomerase-mediated linkage of the elements. The transcribed mRNA was treated with DNaseI (Invitrogen, standard vendor protocol) to degrade the cDNA template. The mRNA was then mixed with lysis buffer, applied to a spin column, washed on the column, and then eluted with pure water (Micro-to-Midi Total RNA purification system, Invitrogen).

First-strand cDNAs were synthesized from P-19 cellular RNA by reverse transcription (20- or 40-μl reaction volume) using the Superscript II (50 U reverse transcriptase per reaction) first-strand synthesis kit (Invitrogen) primed with oligo$(dT)_{12–18}$.

### *Fluorogenic real-time qPCR*

Fluorophore-labeled LUX primers and their unlabeled counterparts were supplied by Invitrogen. LUX

primers were designed by the proprietary software, called LUX Designer (Invitrogen, www.invitrogen.com/lux). Primers and 5′-nuclease probes used for 5′-nuclease assays were designed using Primer Express (Applied Biosystems), and supplied by Biosearch Technologies (Novato, CA).

For P-19 cell experiments, each 20 μl PCR contained 4 μl cDNA (first diluted 1:10 after reverse transcription), 200 nM of each gene-specific primer (two pairs for multiplex PCR) and either 1X Platinum Quantitative PCR SuperMix-UDG (Invitrogen) or Universal Core TaqMan mix (Applied Biosystems, Foster City, CA) including 200 μM each dATP, dGTP, dCTP, and 400 μM dUTP, 1 U uracil DNA glycosylase, 3–3.5 mM $MgCl_2$, 20 mM Tris–HCl, pH 8.4, 50 mM KCl, DNA polymerase antibodies (only in SuperMix-UDG), stabilizers, and *Taq* polymerase (1.5 U *Taq* polymerase in SuperMix-UDG; 1.25 U AmpliTaq Gold polymerase in Universal Master Mix) and 1X ROX reference dye (500 nM in SuperMix). Reactions containing fluorogenic LUX primers included 1X SuperMix and were incubated at 25 °C for 2 min, 95 °C for 2 min, and then cycled (40×) using 95 °C for 15 s, 55 °C for 30 s, and 72 °C for 30 s, and reactions were incubated at 40 °C for 1 min and then ramped to 95 °C over a period of 19 min followed by incubation at 25 °C for 2 min (ramp for melting-curve analysis). Reactions containing 5′-nuclease probes (100 μM) included 1X Universal Core Mix and were incubated at 50 °C for 2 min then at 95 °C for 10 min and then cycled (40×) using 94 °C for 15 s and 60 °C for 30 s. Reactions were conducted in a 96-well spectrofluorometric thermal cycler (ABI PRISM 7700 Sequence detector system, Applied Biosystems). Fluorescence was monitored during every PCR cycle at the annealing or extension step and during the post-PCR temperature ramp.

## Results

### *Differentiation of P-19 cells*

The P-19 mouse embryonic carcinoma cell line is pluripotent and differentiates into neuronal and glial cells in the presence of retinoic acid. The P-19 cells treated with 50 nM retinoic acid formed aggregates (embryoid bodies) within 24 h which then grew larger over the course of the 4-day treatment (Differentiation medium was replaced after 2 days). The embryoid bodies were dissaggregated with a pipetor and vortex and then replated ($1 \times 10^6$ cells per 6-well plate, poly-L-lysine coated) in Differentiation medium lacking retinoic acid. The dissaggregated cells adhered to the culture surface and began sprouting neuron-like processes within 2 h. The processes continued to grow and ramify over the course of a 7-day differentiation period (medium replaced after 4 days). The dissaggregated cells assumed various morphology types resembling neurons or glia, including bipolar cells, stellate cells, and round cells (Fig. 1). Although the induced cultures were enriched in dissaggregated cells, many large, multicell aggregates were still present after dissaggregation, or formed afterward, and grew in size during the 7-day period (not measured). Many cell processes emerged from these aggregates. Total RNA was isolated from cell cultures harvested before the induction period with retinoic acid (Time 0), during the 4-day induction period (1, 6, 48, and 96 h after retinoic acid treatment) and during the differentiation period (1 and 6 h, 1, 3, 5, and 7 days after retinoic acid withdrawal). The resulting RNA yields (measured by absorbance at 260 nM) increased steadily over the time course from 8 to 29 μg per $1 \times 10^6$ million cells plated.

### *LUX primers*

The mono-labeled, fluorogenic LUX primers maintained a self-quenched fluorescence during the early cycles of PCR or when no PCR template was present. The primers then increased their fluorescence intensity when incorporated into double-stranded PCR products. This "LUX effect" is mainly due to the primary sequence of the primer; no quencher is present [14,15]. A G or C base is required at the 3′-end, and one or more Gs are required within 3 bases on the 5′-side of the labeled T-base. A 5′ hairpin tail is added, which forms a

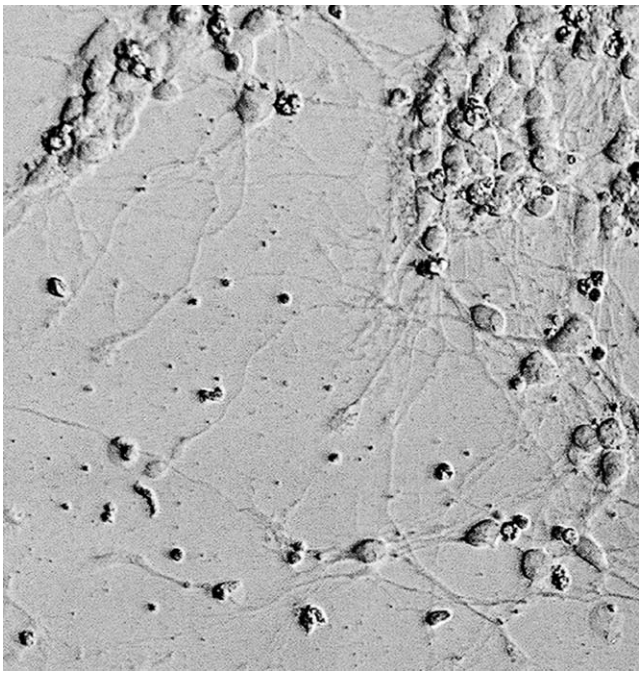

Fig. 1. Differentiated P-19 cells. Cells resembling neurons were photographed (20× objective) 7 days after they were induced to differentiate by retinoic acid treatment.

blunt-end hairpin with a moderate stability ($\Delta G$) at temperatures at or below the planned annealing temperature of PCR. The $\Delta G$ of LUX primers in this study was between −4.3 and −2.7, but may range between −5.5 and −2.5 for the LUX Designer software. Other self-complementarities of LUX primers are avoided. The LUX primers, and their unlabeled counterparts, were designed using a primer design software program called LUX Designer (www.invitrogen.com/lux). Complete coding regions for various genes were obtained from Entrez-PubMed (http://www.ncbi.nlm.nih.gov/entrez/query.fcgi) and pasted into the input field of LUX Designer. The LUX primers were designed to produce amplicons ranging in size between 69 and 145 bp, which was facilitated by resetting the "amplicon size" feature of the LUX Designer program. The melting temperature ($T_m$) of the LUX primers ranged between 60 and 68 °C, which is the default range set by LUX Designer. Several primer pairs located throughout each sequence were designed, and various primer pairs were selected that were located near the 3′-end of the sequence (Table 1). LUX primer pairs were generated for neural gene transcripts that increase during the P-19 blast cell transformation, including neuronal growth-associated protein 43 (GAP-43), glutamate receptor 1 (GLUR1), NMDA-type glutamate receptor 1 (NMDA1), γ-aminobutyric acid receptor B1a (GABA-B1a), choline acetyltransferase, and brain-derived neurotrophic factor (BDNF). Other LUX primer pairs were generated for genes involved in differentiation of neural precursors, including early growth response factor 1 (EGR1), bone morphogenic proteins 2 and 4 (BMP2 and BMP4), and nestin. The LUX primers for all gene targets were labeled with FAM, except LUX primers for a glyceraldehyde-6-phosphate dehydrogenase (GAPDH) target were labeled with JOE. The expression of GAPDH is relatively uniform and its quantitation provides an endogenous reference for the quantitation of variable transcripts.

The real-time PCR amplification efficiency of the LUX primers was first tested before using them to quantify targets in P-19 cells. The efficiencies of the primer sets must be similar to the endogenous reference (GAPDH) in order to validate the relative quantitation method described below. The mRNA from mouse brain was used for this validation because the supply of P-19 cell RNA was limited, and because the expression of some selected genes is low in P-19 cells. The higher copy number of selected genes in brain allows a wide range of input dilutions for generating a standard curve of fluorescence of the PCR cycles versus template amount. The standard curve is done to assess amplification efficiency. Messenger RNA (500 ng) of mouse brain was reverse-transcribed (20-μl reactions) and the resulting cDNA was used for fluorogenic-primer PCR (20 μl reactions in SuperMix, 40 cycles). The 11 target genes were amplified from 25-, 250-, and 2500-fold dilutions of the first-strand cDNA reactions, including 3 replicates per dilution and 3 replicates of no template controls. Plots of fluorescence versus PCR cycle were generated by the ABI PRISM 7700 SDS software. The cycle thresholds ($C_T$), the cycle where the fluorescence rises above

Table 1
Fluorogenic LUX primers pairs used for quantitative RT-PCR

| Target gene | 3′-end | Labeled LUX primer | 3′-end | Unlabeled counterpart | Product |
|---|---|---|---|---|---|
| GABA-B1a (af114168) | 2295 | CACGAACCTTCTTCTCCTCCTTCTTCGTG | 2243 | GCTCTTGGGCTTGGGCTTTAG | 102 |
| GLUR1 (af320126) | 4398 | CACGGTTCCAGATCGTCTTCCTCCGTG | 4349 | GGACGACGATGATGACAGCAG | 97 |
| NMDA1 (nm_008169) | 2569 | CTACGAGTGGCTGGAGGCATCGTAG | 2603 | GGCATCCTTGTGTCGCTTGT | 79 |
| GAP-43 (m16736) | 680 | CACTTTCTGAAGCCAAACCTAAGGAAAGTG | 713 | CAGGCATGTTCTTGGTCAGC | 83 |
| ChAT (d12487) | 683 | CAGCCTCAGTGGGAATGGATTGGCTG | 615 | TCGGCAGCACTTCCAAGACA | 114 |
| BDNF (ay011461) | 729 | GAACATAGCCGAACTACCCAATCGTATGTTC | 759 | CCTTATGAATCGCCAGCCAAT | 82 |
| GAPDH (nm_008084) | 632 | CACGCTCTGGAAAGCTGTGGCGTG | 657 | ACCAGTGGATGCAGGGATGA | 69 |
| EGR1 (nm_007913) | 876 | CAACGAGTAGATGGGACTGCTGTCGTTG | 779 | AGTGGCCTCGTGAGCATGAC | 145 |
| BMP4 (s65032) | 1249 | CACAATGGCTGGAATGATTGGATTGTG | 1288 | CAGCCAGTGGAAAGGGACAG | 86 |
| BMP2 (ay050249) | 5168 | CACCAGTTCTGCGTGGCATGGTG | 5138 | TTGTCTCCTCCTCTGCAAACTCA | 76 |
| Nestin (af076623) | 5798 | CAGCCCAGAGCTTTCCCACGAGGCTG | 5836 | ACCCTGTGCAGGTGGTGCTA | 84 |

Target genes (accession numbers in parentheses) and sequences for LUX primer pairs (given 5′–3′). The 3′-end position is noted due to the nonspecific 5′-tail. Note that the GAP-43 target sequence is for the rat. The bold T designates the labeled base. The size of the PCR product is given.

background (10 times the standard deviation of the background fluorescence), were between 15 and 33 cycles for all PCRs involving all primer sets and template dilutions. A linear relationship exists between the $C_T$ and the initial template concentrations and was plotted (not shown). The correlation ($r^2$) was strong for these linear plots (average $= 0.993 \pm 0.005$ SD, $n = 11$ primer sets). The average slope of the $C_T$ versus initial template plots was $-3.4 \pm 0.17$ SD and the PCR efficiency ($E = 10\exp[-1/\text{slope}]$) ranged between 1.9 and 2.1 (average $= 1.96 \pm 0.06$ SD). The predicted slope and efficiency for 10-fold dilutions is −3.3 and 2, respectively. The efficiency of the GAPDH primer PCR matched that of the other genes, which indicates that relative differences in target genes may be calculated according to the $\Delta\Delta C_t$ mathematical model [19] (User Bulletin 2, Applied Biosystems, 7700 Sequence Detector System, P/N 4303859). The standard criterion for a valid, or matched, set of primer pairs is when the plot of the log of the input amount of template versus the $\Delta C_T$ ($C_T$GAPDH-$C_T$ target gene) has a slope of less than 0.1. This was true for all the target-gene primer sets when compared to GAPDH, except the GABAB1a primer, which showed a slope 0.14.

The average gain of fluorescence above background during real-time PCR was calculated to be $0.5 \pm 0.15$ SD (range 0.73–0.22) for the LUX primer sets. The gain in fluorescence signal during PCR for each primer set was calculated by dividing the difference of the signal plateau (average $4970 \pm 602$ SD, range 6100–4000) and the signal baseline (average $3350 \pm 617$ SD, range 4100–2400) by the signal baseline. All values are relative fluorescence units read from the "multicomponent" plot of the fluorescence versus cycle number (ABI 7700 PRISM).

The PCRs resulted in a single specific product for all LUX primer sets when brain RNA was used as a template for RT-PCR. There was, furthermore, no indication of the inappropriate amplification of nonspecific targets or primer dimers, which may complicate the quantification of target genes. The change in fluorescence versus temperature was plotted for PCR products, for the melting temperature ramp from 40 to 95 °C. The melting curves for all LUX primer PCRs have a single peak, which indicates a single PCR product. There was no signal in the RT-PCR (40 cycles) that did not include cDNA template, which indicates no amplification of primer dimers. Real-time PCR (standard SuperMix 20-μl reactions, 40 cycles) using either mouse brain or liver cDNA (transcribed from mRNA) was performed to check the primer specificity. There was a relatively high, or no, $C_T$ in the RT-PCR that included RNA from liver as the starting template, which indicates the primers are specific. Lastly, agarose-gel analysis of RT-PCRs products from liver and brain samples resulted in a single band of expected size.

*Quantitative RT-PCR using LUX primers*

The level of expression of the selected genes for each time point during P-19 cell development was determined by quantitative, real-time fluorogenic, RT-PCR (qPCR) using a relative method of quantitation (Figs. 2 and 3). The expression of the transcripts, NMDA1, GABA-B1A, GLUR1, GAP-43, and ChAT, substantially increased during the 7-day differentiation period. The increase in BDNF, BMP-2, and BMP-4 transcripts was moderate during the differentiation period, and EGR1 and nestin levels first increased and then decreased. Transcripts levels fluctuated up or down (or both) during the induction period, and most genes increased moderately. The transcription factor EGR1 sharply decreased between the 1- and 6-h time points of both the induction and the differentiation period. For these experiments, the P-19 cell RNA (500 ng) from each time point was reverse-transcribed (40-μl reactions) and the resulting cDNA (4 μl) was used as a template for fluorogenic PCR (40 cycles). PCRs included 4 replicates of cDNA and 4 replicates of no template controls per primer pair. Plots of fluorescence versus PCR cycle were generated by the ABI 7700 SDS software (Fig. 2). The cycle threshold ($C_T$) for a fluorescent PCR correlates with amount of initial template in the PCR. The $C_T$ for the PCRs was between 15 and 32 cycles, except the PCRs for GLUR1 and ChAT, which were between 28 and 38 (not shown). The $C_T$s for GAPDH for all time points ranged between 16.9 and 18.5, which indicate that GAPDH expression was relatively constant. Relative quantification was performed as a relative fold-increase in transcript level with respect to the Time 0 level (preinduction). This method, called comparative $C_T$, does not require plotting a standard curve of $C_T$ versus starting copy number. Instead, the amount of target is calculated based on the difference ($\Delta C_T$) between the average $C_T$ of each time point and the average $C_T$ of the 0-time point. Before subtraction, both $C_T$ values are normalized by subtracting the average $C_T$ of the endogenous reference gene, GAPDH, from each. The $C_T$s for each set of replicates lay within 2 CTs of one another, except in some sets (not measured) in which there was a single outlying replicate. These outlying replicates were attributed to pipeting error or instrument failure at a specific sample well. Thus, the best 3 of 4 replicates were used for relative quantitation in order to exclude outlying replicates from quantitation. The variability among the replicates is expressed as the standard deviation, which ranged from 0.02 to 1.78. The maximum values in the range occurred for PCRs amplifying GLUR1 from early time points, where $C_T$s were relatively high compared to other genes.

Melting-curve analyses indicate that the PCRs produced a single, specific product (Fig. 2C). The change in fluorescence versus temperature was plotted for PCR

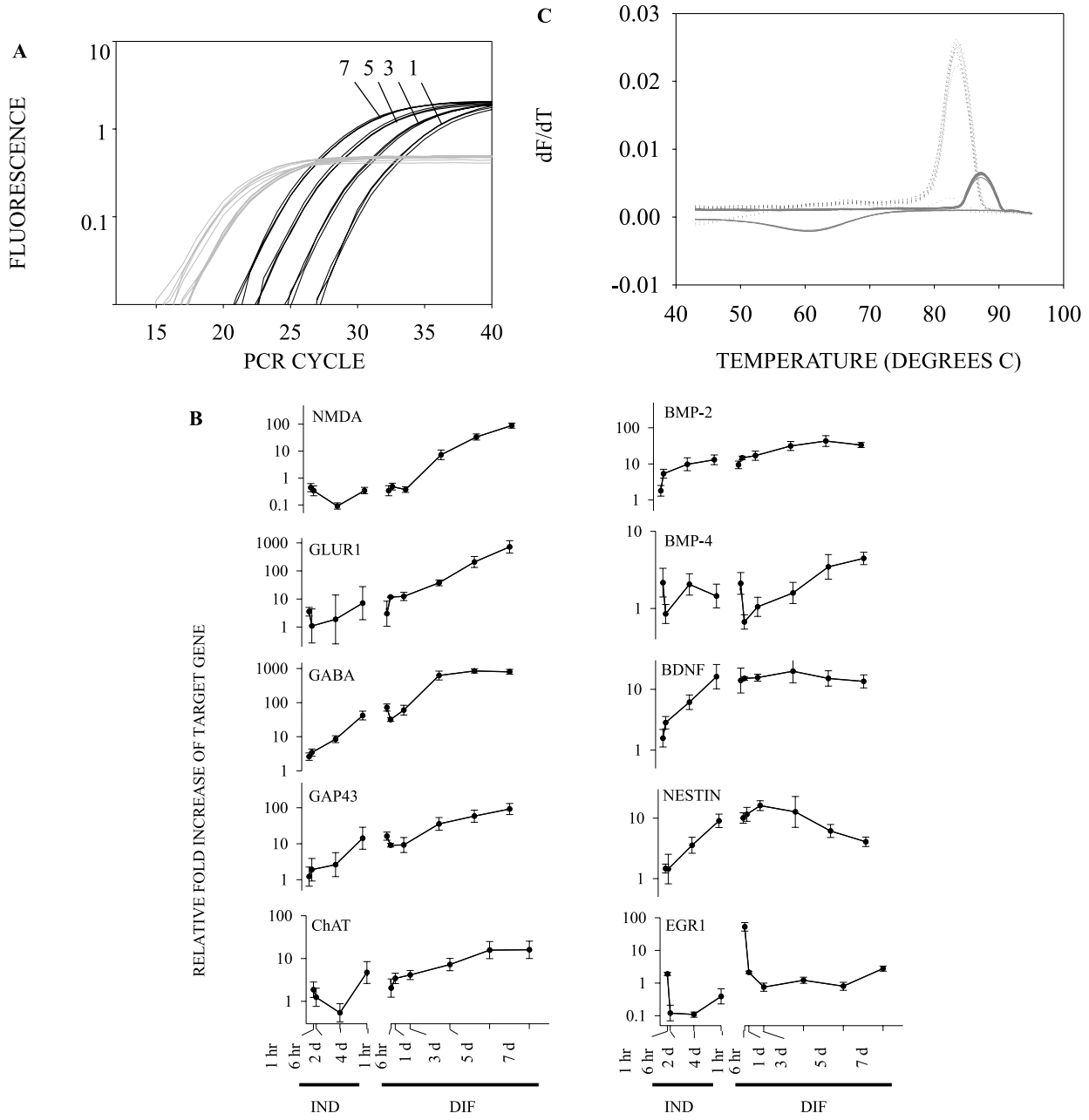


Fig. 2. The time course of gene expression in P-19 cells. (A) Expression of NMDA1 receptor and GAPDH in quantitative RT-PCR samples taken at 1, 3, 5, and 7 days during the differentiation period. The fluorescence versus PCR cycle (3 replicates per time point) is shown for fluorogenic PCRs that amplify transcripts for NMDA1 (dark traces) and GAPDH (light traces) using LUX primers. Higher $C_T$s (points where the traces cross the $x$ axis) are correlated with a lesser amount of initial template. (B) The relative increases in gene expression for several genes in P-19 cells. The comparative $C_T$ method was used to determine the difference in expression between each time point and the 0-time point (before retinoic acid treatment). The expression for samples taken during the 4-day induction period (IND) and the 7-day differentiation period (DIF) is given, and the two periods are separated by a line break. Error bars indicate standard deviation. (C) A representative melting-curve analysis of PCR products. The fluorescence versus temperature for the NMDA and GAPDH PCR products of the experiments shown in A. Each trace is the derivative of the fluorescence versus temperature ($dF/dT$) plot (derivatives calculated using ABI dissociation curve software), which indicates where the plot changes slope and the temperature at which the duplexes melt. One-, 3-, 5-, 7-day samples and no template controls (three replicates each) are shown for NMDA and GAPDH; as in A. Dotted traces are for NMDA and gray traces are for GAPDH. There was a single infection for all melting-curve traces, which indicates a single species of duplex that is assumed to be the specific PCR product. The dips below the baselines occur for PCRs with only LUX primers and are due to changes in secondary structure of the hairpin LUX primers.

products, for the temperature range from 40 to 95 °C in increments of 0.3 °C. This temperature ramp was done after PCR without removing samples from the thermal cycler. This ramp was programmed by SDS 1.7a, ABI 7700 software. PCR with multiple products of various sizes will melt at different temperatures and cause the

slope of the melting curve to have multiple inflections. The melting curves for most LUX primer PCRs have a single inflection, which indicates a single PCR product. An exception occurred for PCRs of ChAT when no cDNA template was added (2 of 4 replicate PCRs). The $C_T$s (average 37.5) for these "no template" reactions were 10 cycles higher than the $C_T$s for reactions including cDNA template. Thus, potential primer-dimer amplification probably contributes little to the ChAT-specific signal. Furthermore, melting-curve analysis indicates that dimers did not form in samples where ChAT cDNA was present, presumably because the cDNA outcompetes potential primer dimers for PCR reactants. Fluorescence for all other PCRs for all genes and time points lacking cDNA did not rise above background.

*In vitro transcription*

ChAT mRNA (903 bp) was generated by in vitro transcription to determine the dynamic range for quantitative real-time RT-PCR, where the approximate initial copy number is known. The transcription reactions yielded 300 ng per reaction (five 20-μl reactions, 100 ng initial template per reaction, were combined) after purification. The optical density of RNA was determined by UV-absorbance measurements, and copy number was then calculated from RNA molecular weight and optical density. The PCR amplification of full-length cDNA, the PCR amplification of the linear, in vitro transcription cDNA construct, and the T7 RNA polymerase reaction all resulted in a single specific product as shown by gel electrophoresis (Fig. 3A). Some very faint bands indicate the presence of nonspecific products, which may induce error in the calculation of the final mRNA copy number of reactions, which induces error in quantitative PCR. Samples of purified ChAT mRNA comprising a 3-fold serial dilution from 66 to $13 \times 10^6$ are discriminated by RT-PCR using LUX primers (Fig. 3B). A linear relationship exists between $C_T$ and starting copy number with high correlation ($r^2 = 0.990$) and a slope of −3.35 (Fig. 3B). The yield of cDNA copies after reverse transcription was not determined. The resulting cDNA (4 μl) from each reverse-transcription reaction was used for separate fluorogenic PCRs with the ChAT primer pair (Table 1). The $C_T$s of the PCRs involving the P-19 cell RNA samples taken at various time points may be compared to the standard curve generated for the in vitro transcribed ChAT mRNA. The average $C_T$s for PCRs involving ChAT were $28.4 \pm 0.55$, $28.5 \pm 0.54$, and $29.9 \pm 0.29$ for the 7, 5, and 3 day time points of the differentiation period, respectively. These $C_T$s correspond to $93.17 \pm 19.94$, $246.07 \pm 84.70$, and $265.52 \pm 88.07$ (average ± SD) initial starting copies of ChAT mRNA. The copies were calculated from the equation of the straight line in the lower graph in Fig. 3B (slope = −3.35; $y$ intercept = 36.5).

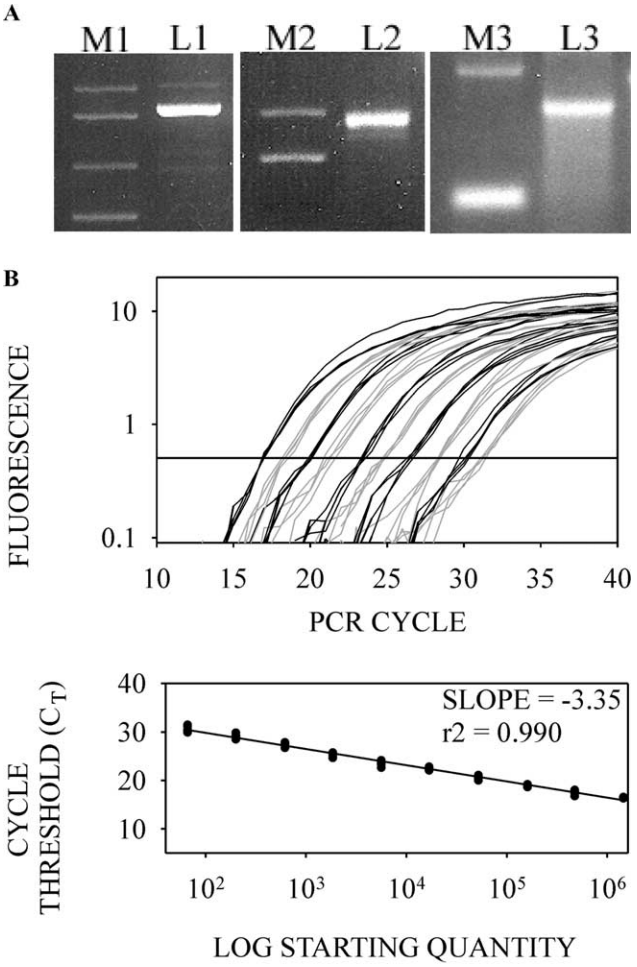


Fig. 3. The RT-PCR of in vitro transcribed ChAT mRNA using LUX primers. (A) Gel analysis of in vitro-transcribed mRNA and its cDNA template. M1, markers (top bands, 850 and 1000 bp); L1, full-length ChAT cDNA (903 bp); M2, markers (top bands, 850 and 1000 bp); L2, ChAT cDNA linked with 5′ T7 and 3′ poly(A) elements (993 bp); M3, markers (1350 and 240 bp); L3, purified ChAT mRNA (993 bp). (B) The fluorescence versus PCR cycle for 3-fold serial dilutions (66–$10^7$ copies) of in vitro-transcribed mRNA (4 replicates per dilution) and standard curve of $C_T$ versus initial RNA template for in vitro-transcribed mRNA. Traces for each of four serial dilution replicates are grouped together and are successively gray then black for each dilution.

*Multiplex LUX and 5′-nuclease assays*

The expression of GLUR1, NMDA1, GAP-43, and ChAT was also quantified by RT-PCR utilizing two sets of LUX primers in the same PCR (multiplex PCR) (Table 1). In the multiplex PCR, one primer set primes a variable neural target using a FAM-labeled primer and the other primes the GAPDH reference target using a JOE-labeled primer. These experiments demonstrate the versatility of the fluorogenic primer PCR assay, especially for use when the input cDNA is in limited supply. The change in the level of expression for the selected genes was similar to the results obtained utilizing a

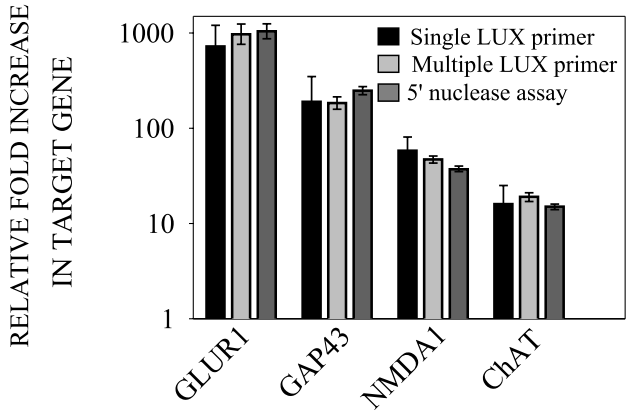


Fig. 4. Comparison of quantitative RT-PCR methods. The relative fold increase between undifferentiated (0 time point) and differentiated (7th day of differentiation) P-19 cells for various genes was calculated using RT-PCR data generated from the use of single LUX primers, multiplex LUX primers, or the 5′-nuclease assay. Error bars show standard deviation.

single LUX primer set (Fig. 4). Both single and multiplex assays used the same cDNA samples from the reverse transcription of RNA harvested at the 0-time point and on the 7th day of the differentiation period. The relative quantitation method (comparative $C_T$) was used to assess the increases in gene expression. The variability among replicates (3 per time point per gene) was slightly higher using a single primer set than for multiplex (Fig. 4).

The result of the single and multiplex, fluorogenic primer PCR assays was confirmed by the more traditional 5′-nuclease hydrolysis-probe assay. The primer and probe sequences are given in Table 2. The cDNA used for the 5′-nuclease assays was the same as for the single and multiplex fluorogenic primer assays. The changes in gene expression between the Time 0 and the 7th day of the differentiation period were comparable between the 5′-nuclease assay and the fluorogenic primer assays (Fig. 4). For Fig. 4, three replicates samples per time point were included for assays of the 5′-nuclease-probe type and the LUX primer type (single and multiplex). All replicates were analyzed for these assays, which were performed separately from the LUX primer assays of Fig. 2. The 5′-nuclease assays had slightly lower variability among replicates than the LUX assays.

Table 2
Primers and probes for 5′-nuclease assays

| Gene | Position | Sequence |
|---|---|---|
| GAPDH | F-5′-251 | gggaagcccatcaccatctt |
| | R-3′-326 | cgacatactcagcaccggc |
| | P-5′-276 | ttcctacccccaatgtgtccgtcgt |
| ChAT | F-5′-598 | ggcagcacttccaagacacc |
| | R-3′-673 | gccttgtagctaagcacaccaga |
| | P-5′-620 | catcgtggcctgctgcaacca |
| GAP-43 | F-5′-712 | ggctgaccaagaacatgcct |
| | R-3′-787 | ggcaggagagacagggttca |
| | P-5′-744 | ttccacgttgcccccacctga |
| GLUR1 | F-5′-2405 | agcgcctcctagttggcct |
| | R-3′-2480 | atgcgtgcaatacgattggtt |
| | P-5′-2426 | caggtggaagacaggcgccca |
| NMDA1 | F-5′-2555 | ctggaggcatcgtagctgg |
| | R-3′-2630 | ttcctacgggcatccttgtg |
| | P-5′-2582 | tgttcttccgctccggctttgg |

Sequences are written 5′–3′. All PCR products are 75 bp. F, forward primer; R, reverse primer; P, probe.

## Discussion

Quantitative, real-time, RT-PCR using LUX primers was used to rapidly and reliably quantify the relative level of expression of multiple genes as their levels fluctuated during P-19 cell differentiation. The PCRs using LUX primers yielded robust data that were applied to the comparative $C_T$ method for calculating the change in the relative expression between samples. Several patterns of expression existed for the selected transcripts. The neuronal-associated genes, NMDA, GLUR1, GABA-B1a, and GAP-43 increased between 100- and 1000-fold during the 7-day differentiation period. The increases in NMDA1 and GluR1 are consistent with other experiments that investigate changes in the levels of expression of these genes in P-19 cells [27,28]. The increase in expression of GABA-A receptors was reported in differentiated P-19 cells [29], and GABA-B receptors were characterized [30] and found to be expressed in neurons [31]. This is the first known report of increased GABA-B1a expression in differentiated P-19 cells. The GAP-43 protein reached high levels in differentiated P-19 cells after 8 days in culture [32]. We show a complementary increase in GAP-43 transcript that precedes the high level of protein expression reported. Furthermore, we provide relative quantitation of the increase in expression.

The increase in the neuronal gene, ChAT, was approximately 10-fold. This increase is relatively low compared to the other neuronal genes, and may result from a low number of P-19 cells that transformed into cholinergic neurons, compared to GABAergic or glutamatergic neurons. The number of cholinergic P-19 cells induced by retinoic acid is dependent upon the culture density of P-19 cells, whereas cell density has no affect on the number of glutamatergic and gabaergic cells [33]. The density of P-19s in culture was not measured in this study.

The genes BMP-2 and -4 increased approximately 10-fold, and most of this increase occurred during the 4-day induction period. The BMP-2 and -4 proteins are produced in undifferentiated cells and may act synergistically with retinoic acid to induce astroglia differentiation in P-19 cells [34]. The neurotrophic factor, BDNF, also increased approximately 10-fold during the induction

period of our experiments. BDNF receptors are expressed in neural precursors [35] and BDNF plays a role in neurogenesis [36]. The type of cells, e.g., neurons, glia, stem, or other, expressing BMP-2 and -4 was not identified in these experiments. Additional work to identify the expression pattern of the various cell types in these cultures may be useful for future studies of P-19 cell differentiation. The spike in EGR1 expression that we report is consistent with previous reports that demonstrate EGR1 (Krox 24) is expressed early during differentiation of P-19 cells, and that EGR1 plays a role in differentiation [37]. Nestin, also implicated in P-19 differentiation, increased during the 4-day induction period. Previous reports also demonstrate that the expression of nestin protein rises and then falls with a similar time course as in this study [38]. Whether the changes in expression reported in this study are involved in differentiation is beyond the scope of this report. The results, nonetheless, are valid and may provide useful data for further studies on the role of gene expression during neurogenesis.

The linkage of TOPO-charged elements, a 5′-T7 promoter and a 3′ poly(A) tail, to full-length cDNA by topoisomerase-mediated reactions is a rapid and easy method to create mRNA that may be used to generate a standard curve for real-time RT-PCR. Real-time, RT-PCR using LUX primers quantifies approximately 3-fold changes in the amount of in vitro-transcribed ChAT mRNA over the dynamic range between 66 and $1 \times 10^7$ transcripts per reverse-transcription reaction. The plot of $C_T$ versus log of initial mRNA starting amount is highly correlative ($r^2 = 0.990$ and slope $= -3.35$). This type of plot may be used as a standard "calibration" curve for quantitative, real-time, RT-PCR. For instance, the $C_T$s obtained from unknown samples may then be compared to the standard curve to estimate the absolute copy number of the unknown samples. The standard curve generated for ChAT (Fig. 3B) indicates that a $C_T$ of 31 represents 60 to 70 copies. We note that our experiments were not sufficiently replicated to provide a precise measure of absolute copy number [11].

The quantitation of two transcripts in the same PCR reaction (multiplex PCR) was attainable using two LUX primer pairs per reaction, with each LUX primer having a separate emission wavelength maximum. One LUX primer was labeled with FAM and used to quantify a variable target, and the other was labeled with JOE and used to quantify the endogenous reference (GAPDH, a housekeeping gene). The quantification of transcripts in P-19 cells using multiplex PCR yielded similar results to quantification using PCRs with a single primer set per reaction. We are currently investigating how well other common fluorophores perform as LUX primers.

The LUX primer pairs used for the experiments were easily designed using the proprietary software (LUX Designer; Invitrogen), and the use of the LUX primers, including multiplex applications, required no optimization of the PCR cycling parameters or reagent concentrations. The LUX primer design is flexible and therefore may be adjusted to amplify regions of transcripts that span exon-exon boundaries. We chose to use primer sets that amplified sequences near the 3′-end of the coding regions. This strategy is useful when using oligo(dT) to prime reverse transcription. The design flexibility for LUX primers may be useful when creating a qPCR assay for highly mutated targets or for assays that target genes with multiple spliceforms. Most LUX primers amplified their targets with efficiency comparable to GAPDH and the comparative $C_T$ method was used for relative quantitation. If, however, a LUX primer set and the endogenous reference set have greatly different efficiency, another LUX primer set may be designed. This new primer set may include the same LUX primer sequence paired with a different unlabeled primer sequence, or may have different LUX primer. An alternative is to use other mathematical models that factor the PCR efficiencies of both primer sets when quantifying relative differences in transcripts [26]. Quantitation by the calibration-curve method is another alternative [11,26]. A potential drawback of using LUX primers for RT-PCR is the possible amplification and detection of nonspecific products, primer dimers or incomplete products, which may result in false positives, overestimates of input DNA, or variability among replicate samples. The detection of PCR artifacts may be less likely when using a probe-based method. However, the use of antibody-based "hotstart" PCR and the hairpin structure of the LUX primer [14,39,40] may help avoid these PCR artifacts. Furthermore, primer-dimer amplification is rare when specific template is present in the PCR (unpublished observation). We conclude that quantitative, real-time RT-PCR using fluorogenic LUX primers is a reliable, cost-effective alternative for investigating the expression of multiple genes in neural stem cells.

## Acknowledgments

We thank Joseph Hayes and Rick Pires for primer synthesis. David Saile of Invitrogen Corp. programmed the LUX Designer program.

## References

[1] S.C. Zhang, M. Wernig, I.D. Duncan, O. Brustle, J.A. Thomson, In vitro differentiation of transplantable neural precursors from human embryonic stem cells, Nat. Biotechnol. 12 (2001) 1129–1133.

[2] J.H. Kim, J.M. Auerbach, J.A. Rodriguez-Gomez, I. Velasco, D. Gavin, N. Lumelsky, S.H. Lee, J. Nguyen, R. Sanchez-Pernaute, K. Bankiewicz, R. McKay, Dopamine neurons derived from

embryonic stem cells function in an animal model of Parkinson's disease, Nature 418 (2002) 50–56.
[3] K. D'Amour, F.H. Gage, New tools for human developmental biology, Nat. Biotechnol. 18 (2000) 381–382.
[4] A.Y. Hung, E.H. Koo, C. Haass, D.J. Selkoe, Increased expression of β-amyloid precursor protein during neuronal differentiation is not accompanied by secretory cleavage, Proc. Natl. Acad. Sci. USA 89 (1992) 9439–9443.
[5] S. Aronov, G. Aranda, L. Behar, I. Ginzburg, Axonal tau mRNA localization coincides with tau protein in living neuronal cells and depends on axonal targeting signal, J. Neurosci. 21 (2001) 6577–6587.
[6] Z. Cao, Y. Wang, E.A. Reid, G. McShepard, M. Kemp, R.F. Newkirk, J.G. Townsel, The quantitative distribution of a putative PKC epsilon mRNA in Limulus central nervous system by modified competitive RT-PCR, J. Neurosci. Methods 105 (2001) 193–199.
[7] A.C. Grobin, A.L. Morrow, 3α-hydroxy-5α-pregnan-20-one levels and GABA(A) receptor-mediated 36Cl(-) flux across development in rat cerebral cortex, Brain Res. Dev. Brain Res. 131 (2001) 31–39.
[8] C.F. Peng, Y. Wei, J.M. Levsky, T.V. McDonald, G. Childs, R.N. Kitsis, Microarray analysis of global changes in gene expression during cardiac myocyte differentiation, Physiol. Genomics 9 (2002) 145–155.
[9] S. Anisimov, K. Tarasov, D. Riordon, A. Wobus, K. Boheler, SAGE identification of differentiation responsive genes in P19 embryonic cells induced to form cardiomyocytes in vitro, Mech. Dev. 117 (2002) 25.
[10] Y. Yamauchi, S. Hongo, T. Ohashi, S. Shioda, C. Zhou, Y. Nakai, N. Nishinaka, R. Takahashi, F. Takeda, M. Takeda, Molecular cloning and characterization of a novel developmentally regulated gene, Bdm1, showing predominant expression in postnatal rat brain, Brain Res. Mol. Brain Res. 68 (1999) 149–158.
[11] S.A. Bustin, Absolute quantification of mRNA using real-time reverse transcription polymerase chain reaction assays, J. Mol. Endocrinol. 25 (2000) 169–193.
[12] C.A. Heid, J. Stevens, K.J. Livak, P.M. Williams, Real time quantitative PCR, Genome Res. 10 (1996) 986–994.
[13] W.M. Freeman, S.J. Walker, K.E. Vrana, Quantitative RT-PCR: pitfalls and potential, Biotechniques 26 (1999) 112–122, 124–125.
[14] I. Nazarenko, B. Lowe, M. Darfler, P. Ikonomi, D. Schuster, A. Rashtchian, Multiplex quantitative PCR using self-quenched primers labeled with a single fluorophore, Nucleic Acids Res. 30 (2002) 37.
[15] I. Nazarenko, R. Pires, B. Lowe, M. Obaidy, A. Rashtchian, Effect of primary and secondary structure of oligodeoxyribonucleotides on the fluorescent properties of conjugated dyes, Nucleic Acids Res. 30 (2002) 2089–2195.
[16] I.A. Nazarenko, S.K. Bhatnagar, R.J. Hohman, A closed tube format for amplification and detection of DNA based on energy transfer, Nucleic Acids Res. 25 (1997) 2516–2521.
[17] S. Tyagi, F.R. Kramer, Molecular beacons: probes that fluoresce upon hybridization, Nat. Biotechnol. 3 (1996) 303–308.
[18] L.G. Lee, C.R. Connell, W. Bloch, Allelic discrimination by nick-translation PCR with fluorogenic probes, Nucleic Acids Res. 21 (1993) 3761–3766.
[19] P.M. Holland, R.D. Abramson, R. Watson, D.H. Gelfand, Detection of specific polymerase chain reaction product by utilizing the 5′–3′ exonuclease activity of *Thermus aquaticus* DNA polymerase, Proc. Natl. Acad. Sci. USA 88 (1991) 7276–7280.
[20] C.T. Wittwer, M.G. Herrmann, A.A. Moss, R.P. Rasmussen, Continuous fluorescence monitoring of rapid cycle DNA amplification, Biotechniques 1 (1997) 130–131, 134–138.
[21] R. Higuchi, C. Fockler, G. Dollinger, R. Watson, Kinetic PCR analysis: real-time monitoring of DNA amplification reactions, Biotechnology (NY) 9 (1993) 1026–1030.
[22] N. Thelwell, S. Millington, A. Solinas, J. Booth, T. Brown, Mode of action and application of Scorpion primers to mutation detection, Nucleic Acids Res. 19 (2000) 3752–3761.
[23] M. Kotani, T. Osanai, Y. Tajima, H. Kato, M. Imada, H. Kaneda, H. Kubo, H. Sakuraba, Identification of neuronal cell lineage-specific molecules in the neuronal differentiation of P19 EC cells and mouse central nervous system, J. Neurosci. Res. 67 (2002) 595–606.
[24] G. Bain, D.I. Gottlieb, Neural cells derived by in vitro differentiation of P19 and embryonic stem cells, Perspect. Dev. Neurobiol. 5 (1998) 175–178.
[25] M.W. McBurney, E.M. Jones-Villeneuve, M.K. Edwards, P.J. Anderson, Control of muscle and neuronal differentiation in a cultured embryonal carcinoma cell line, Nature 299 (1982) 165–167.
[26] M.W. Pfaffl, A new mathematical model for relative quantification in real-time RT-PCR, Nucleic Acids Res. 29 (2001) E45–E45.
[27] E.R. Grant, M.A. Errico, S.L. Emanuel, D. Benjamin, M.K. McMillian, S.A. Wadsworth, R.A. Zivin, Z. Zhong, Protection against glutamate toxicity through inhibition of the p44/42 mitogen-activated protein kinase pathway in neuronally differentiated P-19 cells, Biochem. Pharmacol. 62 (2001) 283–296.
[28] S. Heck, R. Enz, C. Richter-Landsberg, D.H. Blohm, Expression of eight metabotropic glutamate receptor subtypes during neuronal differentiation of P-19 embryocarcinoma cells: a study by RT-PCR and in situ hybridization, Brain Res. Dev. Brain Res. 101 (1997) 85–91.
[29] A. Grobin, J.R. Chistina, R.D. Inglefield, L.L. Schwartz-Bloom, A.L. Devaud Morrow, Fluorescence imaging of GABAA receptor-mediated intracellular [Cl-] in P-19-N cells reveals unique pharmacological properties, Brain Res. 827 (1999) 1–11.
[30] R. Sullivan, A. Chateauneuf, N. Coulombe, L.F. Kolakowski Jr., M.P. Johnson, T.E. Hebert, N. Ethier, M. Belley, K. Metters, M. Abramovitz, G.P. O'Neill, G.Y. Ng, Coexpression of full-length γ-aminobutyric acid(B) (GABA(B)) receptors with truncated receptors and metabotropic glutamate receptor 4 supports the GABA(B) heterodimer as the functional receptor, J. Pharmacol. Exp. Ther. 293 (2000) 460–467.
[31] S. Towers, A. Princivalle, A. Billinton, M. Edmunds, B. Bettler, L. Urban, J. Castro-Lopes, N.G. Bowery, GABAB receptor protein and mRNA distribution in rat spinal cord and dorsal root ganglia, Eur. J. Neurosci. 12 (2000) 3201–3210.
[32] S. Mani, J. Schaefer, K.F. Meiri, Targeted disruption of GAP-43 in P-19 embryonal carcinoma cells inhibits neuronal differentiation, Brain Res. 853 (2000) 384–395.
[33] D. Parnas, M. Linial, Acceleration of neuronal maturation of P-19 cells by increasing culture density, Brain Res. Dev. Brain Res. 101 (1997) 115–124.
[34] M. Bani-Yaghoub, J.M. Felker, C. Sans, C.C. Naus, The effects of bone morphogenetic protein 2 and 4 (BMP2 and BMP4) on gap junctions during neurodevelopment, Exp. Neurol. 162 (2000) 13–26.
[35] V.L. Sheen, M.W. Arnold, Y. Wang, J.D. Macklis, Neural precursor differentiation following transplantation into neocortex is dependent on intrinsic developmental state and receptor competence, Exp. Neurol. 158 (1999) 47–62.
[36] M. Barbacid, Neurotrophic factors and their receptors, Curr. Opin. Cell Biol. 7 (1995) 148–155.
[37] J. Lanoix, A. Mullick, Y. He, R. Bravo, D. Skup, Wild-type egr1/Krox24 promotes and dominant-negative mutants inhibit, pluripotent differentiation of P-19 embryonal carcinoma cells, Oncogene 17 (1998) 2495–2504.
[38] P. Lin, K. Kusano, Q. Zhang, C.C. Felder, P.M. Geiger, L.C. Mahan, GABAA receptors modulate early spontaneous excitatory activity in differentiating P-19 neurons, J. Neurochem. 66 (1996) 233–242.

[39] D.J. Sharkey, E.R. Scalice, K.G. Christy Jr., S.M. Atwood, J.L. Daiss, Antibodies as thermolabile switches: high temperature triggering for the polymerase chain reaction, Biotechnology (NY) 12 (1994) 506–509.

[40] M. Ailenberg, M. Silverman, Controlled hot start and improved specificity in carrying out PCR utilizing touch-up and loop incorporated primers (TULIPS), Biotechniques 5 (2000) 1018–1020, 1022–1024.